

## MODELLING OF GEOSYNTHETIC REINFORCED RAILWAY TRACKS RESTING ON SOFT CLAYS

S. Rajesh<sup>1</sup>, K. Choudhary<sup>2</sup>, and S. Chandra<sup>3\*</sup>

<sup>1</sup>Assistant Professor, Department of Civil Engineering, Indian Institute of Technology Kanpur, Kanpur, India; Tel: +91 542 259 6054; Fax: +91 542 259 7395; Email: hsrajesh@iitk.ac.in.

<sup>2</sup>Former Post Graduate Student, Department of Civil Engineering, Indian Institute of Technology Kanpur, Kanpur, India; Email: ckirti@iitk.ac.in

<sup>3</sup>Professor, Department of Civil Engineering, Indian Institute of Technology Kanpur, Kanpur, India; Tel: +91 542 259 7667; Fax: +91 542 259 7395; Email: sarv@iitk.ac.in. (\*corresponding author)

### ABSTRACT

The objective of this paper is to develop a foundation model which idealizes a ballasted railway track along with geosynthetic reinforcement considering soft clay as founding soil. The suggested foundation model incorporated various aspects of the behavior of geosynthetic reinforced ballasted track system which become quintessential in field situations. Some of the aspects include time dependent behavior of soft subgrade, compressibility of ballast and sub-ballast layers and predicting settlement at desired instants of time. The model uses a rough stretched elastic membrane to idealize the behavior of the geosynthetic layer. The burger model has been used to characterize the soft viscoelastic subgrade. Numerical solutions have been obtained by adopting the finite difference method combined with non-dimensionalizing the governing equations of the proposed model. It was observed that at a wheel load of 250 tonnes, there is a reduction of 4.9% in the settlement of the reinforced system when compared with the settlement values of the unreinforced system. The reduction in the settlement is due to the mobilized tensile load of geosynthetic provided in between ballast and sub-ballast layers. This study reveals that the geosynthetic reinforcement can play a major role in reducing the track settlements and thereby improving the current unreinforced ballasted railway tracks by increasing their efficiency.

*Keywords: Railway track system, geosynthetics, pasternak shear layer, burger model, settlement*

### INTRODUCTION

Railway tracks (rails and sleepers) are normally laid on a sub-structure that consists of two or more layers of different materials. The top layer (below the sleepers) is a layer of railway ballast. Below the ballast there might be layers of sub-ballast, a formation layer and/or the subgrade. The ballast bed consists of loose, coarse grained materials which are capable of absorbing considerable dynamic compressive stresses due to internal friction between the grains. The substructure or subgrade must possess sufficient bearing strength and must display reasonable settlement behavior. However, when the subgrade is soft clay or when the softening of the subgrade occurs, then track alignment and track level might deteriorate. To prevent such situations, new developments have found their way into the design of traditional ballasted track. One such development is the use of geosynthetic layer between the ballast and sub-ballast layer. The inclusion of reinforcing layers offers advantages in the form of high design loads as well as significant reduction in track maintenance. Geosynthetic layers also prevent particle migration at the ballast and sub-ballast interface and prevent mud pumping.

The performance of a railway track depends to a large extent on how the large, concentrated wheel loads is transferred to the subgrade. A well-designed and constructed track would distribute the loads in a relatively uniform fashion, without overstressing any of the track components: rail, sleepers, ties, ballast and subgrade. When a wheel is centered over a sleeper, less than half of the load is carried by the sleeper directly beneath the wheel, while rest of the load is distributed among the neighboring two sleepers (Beranek 2000). The applied load on the sleeper will be transferred to ballast layer which in-turn to sub-ballast and subgrade layers. While determining the net effect of wheel loads on the track structure, the track model should be able to inter-relate the components of the track structure in a way such that their complex interactions are properly taken into consideration. Such a model would then provide a means for predicting track settlements and hence, the technical and economic feasibility of the track design.

Theoretical model used for idealizing a railways track should be capable of including the effects of sleeper spacing, rail stiffness, changes in ballast and sub-ballast thickness and subgrade properties. The

simplest representation of a track structure can be described as a beam resting on an elastic foundation wherein the substructure is represented by a Winkler spring system. However, such a system will not be able to quantify the individual contributions of ballast, sub-ballast and subgrade in much detail. This made several researchers to develop various foundation models. Even though foundation models representing the behavior of geosynthetic reinforced soil system have been developed by many researchers, the applications of these models for studying railway track behavior has not been considered in the past studies. Hence, in the present study, a foundation model which idealizes a geosynthetic based ballasted railway track resting on soft clay was developed by combining various lumped parameter models.

### STATEMENT OF THE PROBLEM

A typical layout of geosynthetic reinforced railway track is shown in Fig. 1. It comprises of rail, sleepers, ballast layer, geosynthetic layer, sub-ballast layer and soft subgrade layer. The proposed foundation model which idealizes the behavior of such a railway track system is shown in Fig. 2. In the proposed model, the ballast and sub-ballast layers have been idealized by Pasternak shear layer. Pasternak shear layer is a two parameter model consisting of a shear layer of unit thickness above the Winkler springs to account for the compressibility and shear interaction between the spring elements. To incorporate the compressibility of both ballast and sub-ballast layer, a layer of stiff Winkler springs has been connected to the bottom of the lower Pasternak shear layer. The shear layers are made up of incompressible vertical elements which deforms only in transverse shear. The geosynthetic layer is represented by a stretched rough elastic membrane. While deriving the settlement response of this system, it was assumed that geosynthetic layer is linearly elastic with negligible shear resistance and does not allow slippage at the interface due to its roughness. A rigid perfectly plastic friction model has been adopted to represent the soil-geosynthetic interface in shear. Further it was assumed that the displacement of the membrane is zero at the instant when the load is applied and the deformation takes place only after application of the load.

Many studies have indicated that incorporation of the reinforcement affects the stress-strain distribution within the system. In order to quantify the effect of geosynthetic layer, the tensile stresses mobilized in the reinforcement has been considered. These tensile forces are an outcome of the accumulated frictional forces acting along the entire length of the inclusion. This whole phenomenon is

popularly known as the “Rough Membrane Effect” of the geosynthetic reinforcement. The induced shear stresses due to the geosynthetic layer also cause confinement of the soil in the neighboring environment of the inclusion. Soft soil subgrade has been idealized with four parameter Burger model. The adopted Burger model is a combination of Kelvin-Voigt element and Maxwell element arranged in series. Burger model has been adopted because of the flexibility it provides and also depicts the behavior of soft clay closely.

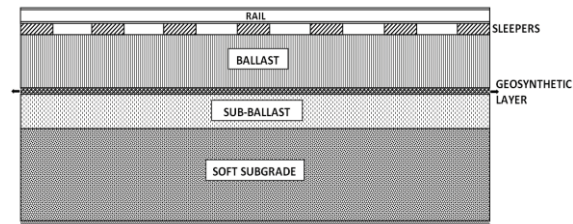


Fig. 1 Typical layout of a geosynthetic reinforced railway track

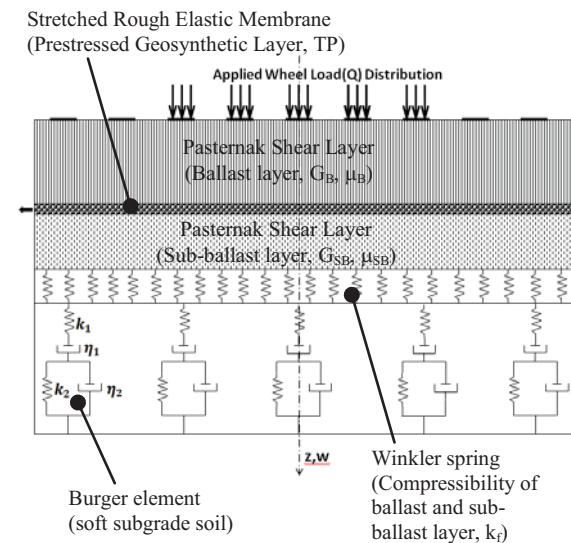


Fig. 2 Schematic diagram of proposed foundation model

### SETTLEMENT AND MOBILISED TENSILE RESPONSE OF THE MODEL

The settlement response of the proposed model has been arrived by applying uniformly distributed load with intensity  $q$ , over a length  $2B$ , directly on the top of the ballast layer. As per Beranek (2000), the total wheel load  $Q$  for a unique static position of the train is spread to the sleepers as shown in Fig. 3. The total width of the sleeper ( $2B$ ) is the summation of the effective sleeper widths within which the load is being applied for a unique static position of the

train. In the analysis, the total wheel load from the train wheel has been appropriately modified to the stresses intensity  $q$  transferred to the sleepers considering suggested load distribution. Plane strain conditions are considered for both the loading and the foundation soil system. This is due to the fact that the length of the sleeper is quite large in comparison to the width of the sleeper ( $\frac{L_{sleeper}}{W_{sleeper}} \approx 8 - 9$ ). As a result, the applied forces would not vary along the length i.e. loads are uniformly distributed with respect to the larger dimension (in this case length of the sleeper) and act perpendicular to it as well.

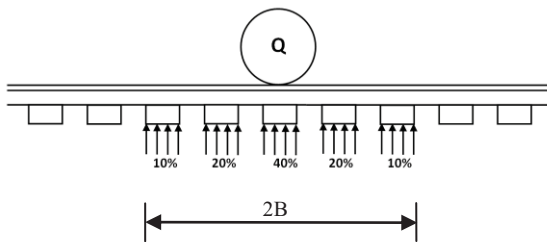


Fig. 3 Wheel load distribution (Beranek, 2000)

The following assumptions are made while deriving the equations:

1. Plane strain conditions exist for both the loading and foundation soil system.
2. Downward deflection is positive and loading acting in downward direction is also positive.
3. Shear force on the left side of a section is positive in upward direction and consequently on the right side, it is positive in downward direction.
4. Due to symmetric loading conditions, it is sufficient to analyze only one half of the loading.

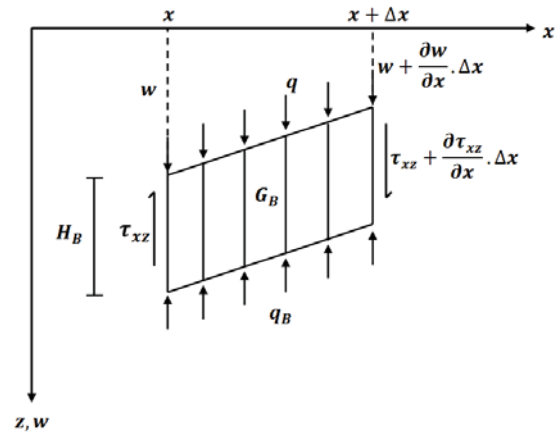
The governing equations for the settlement response have been derived by considering first an element of the ballast shear layer and its vertical force equilibrium has been studied. Once this is done, the geosynthetic reinforcement represented by the rough elastic membrane is considered. Once the horizontal and vertical force equilibrium for the membrane element has been established, equations relating to the vertical force equilibrium of an element of the sub-ballast shear layer have been established. The stress distribution and the force distribution of the ballast shear layer is given in Fig. 4.

It is assumed that the shear layer parameter,  $G$  is isotropic in the  $x$ - $y$  plane, which implies,

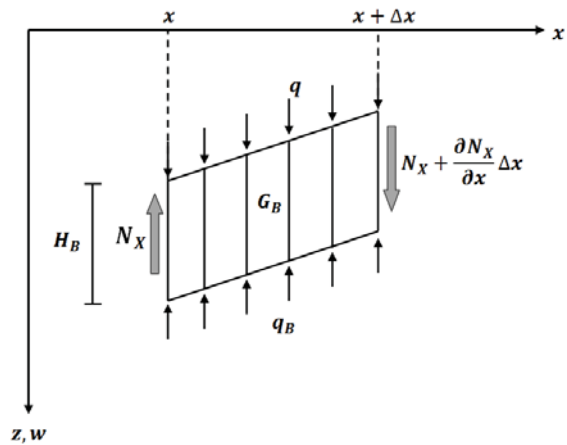
$$G_x = G_y = G_B \quad (1)$$

$$\tau_{xz} = G_B \gamma_{xz} = G_B \frac{\partial w}{\partial x} \quad (2)$$

where  $G_B$  is the shear parameter of the ballast shear layer.



a) Free-body diagrams of ballast shear layer subjected to stresses



b) Free-body diagrams of ballast shear layer subjected to forces

Fig. 4 Free-body diagrams of ballast shear layer subjected to stresses and forces

Total shear force is obtained by integrating equation 2 over the depth  $H_B$ ,

$$N_x = \int_0^{H_B} \tau_{xz} dz = \int_0^{H_B} G_B \frac{\partial w}{\partial x} dz = G_B H_B \frac{\partial w}{\partial x} \quad (3)$$

where  $H_B$  is the height of the ballast layer.

Considering the vertical equilibrium of the forces acting on the ballast shear layer, it turns out that,

$$\frac{\partial N_x}{\partial x} + q - q_B = 0 \quad (4)$$

where  $q_B$  is the vertical force interaction between ballast and membrane. Substituting equation 3 in the above equation, the following relation is obtained,

$$q = q_B - G_B H_B \frac{\partial^2 w}{\partial x^2} \quad (5)$$

The effect of transverse shear interactions can be seen in the second term on the right hand side of equation 5.

Figure 5 shows the force equilibrium for the stretched rough elastic membrane. The horizontal force equilibrium equation for this membrane can be written as,

$$(T_p + T + \Delta T) \cos(\theta + \Delta\theta) - (T_p + T) \cos \theta + (\mu_B q_B + \mu_{SB} q_{SB}) \Delta x + K(q_B - q_{SB}) \Delta x \tan \theta = 0 \quad (6)$$

where,  $q_{SB}$  is the vertical force interaction between the membrane and the sub-ballast layer,  $\mu_B$  and  $\mu_{SB}$  are the interface friction coefficients at the top and bottom faces of the membrane respectively,  $\theta$  is the slope of the membrane,  $T(x)$  is the tensile force per unit length mobilised in the membrane,  $T_p$  is the pretension per unit length applied to the membrane and  $K$  is the coefficient of lateral stress.  $K$  is the ratio of horizontal to vertical stresses present in the granular fill. If the developed stresses within the fill are the maximum ever developed in the stress history, the reinforced granular fill is at a  $K_0$  (coefficient of lateral stress at rest) state of stress. However, for an over consolidated fill,  $K$  is greater than  $K_0$ , hence, in such conditions the relationship suggested by Alpan (1967) is used,

$$K = K_0 R_c^\lambda \quad (7)$$

where,  $R_c$  is the over consolidation ratio and  $\lambda$  is rest-rest rebound exponent which can be correlated with the effective angle of shearing resistance ( $\phi'$ ) (Sukla, 1995).  $K_0$  is the coefficient of earth pressure at rest which can be determined by the relation,  $K_0 = 1 - \sin \phi'$

Now, taking the limit that  $\Delta x \rightarrow 0$  in equation 5, the following equation is obtained,

$$\cos \theta \frac{\partial T(x)}{\partial x} - (T_p + T) \sin \theta \frac{\partial \theta}{\partial x} = -(\mu_B q_B + \mu_{SB} q_{SB}) + K(q_B - q_{SB}) \tan \theta \quad (8)$$

The vertical force equilibrium for the stretched rough elastic membrane yields the following equation,

$$(T_p + T + \Delta T) \sin(\theta + \Delta\theta) - (T_p + T) \sin \theta - (q_B - q_{SB}) \Delta x + K(\mu_B q_B + \mu_{SB} q_{SB}) \Delta x \tan \theta = 0 \quad (9)$$

Taking the limit,  $\Delta x \rightarrow 0$ , the equation 9 reduces to,

$$\sin \theta \frac{\partial T(x)}{\partial x} + (T_p + T) \cos \theta \frac{\partial \theta}{\partial x} = (q_B - q_{SB}) - K(\mu_B q_B + \mu_{SB} q_{SB}) \tan \theta \quad (10)$$

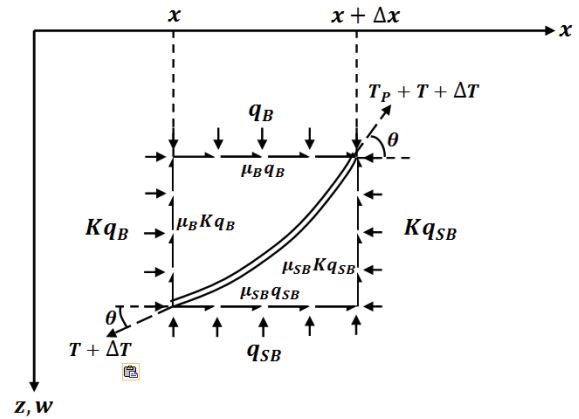


Fig. 5 Free-body diagram of geosynthetic layer (membrane element) subjected to forces

Combining equations 8 and 10 and simultaneously eliminating the differential term in  $T(x)$ ,

$$q_B = q_{SB} + \frac{(T_p + T) \sec \theta \frac{\partial \theta}{\partial x}}{1 + K \tan^2 \theta} - \frac{(1 - K)(\mu_B q_B + \mu_{SB} q_{SB}) \tan \theta}{1 + K \tan^2 \theta} \quad (11)$$

$\theta$  is written in terms of vertical displacement,  $w(x)$ , as follows,

$$\tan \theta = \frac{dw}{dx} \quad (12)$$

Differentiating equation 12 with respect to  $x$ , equation 13 can be obtained,

$$\sec^2 \theta \frac{d\theta}{dx} = \frac{d^2 w}{dx^2} \quad (13)$$

Substituting equation 12 and 13 into equation 11, the following equation is obtained,

$$q_B = \bar{X}_1 q_{SB} - \bar{X}_2 (T_p + T) \cos \theta \frac{\partial^2 w}{\partial x^2} \quad (14)$$

where,

$$\bar{X}_1 = \frac{1 + K \tan^2 \theta - (1 - K) \mu_{SB} \tan \theta}{1 + K \tan^2 \theta + (1 - K) \mu_r \tan \theta} \quad (15)$$

and

$$\bar{X}_2 = \frac{1}{1 + K \tan^2 \theta + (1 - K) \mu_r \tan \theta} \quad (16)$$

Figure 6 show the stress distribution for the sub-ballast shear layer element. The same assumption of isotropic shear parameter is taken here as well, which results in the following governing equation for the sub-ballast shear layer element,

$$q_{SB} = q_s - G_{SB} H_{SB} \frac{\partial^2 w}{\partial x^2} \quad (17)$$

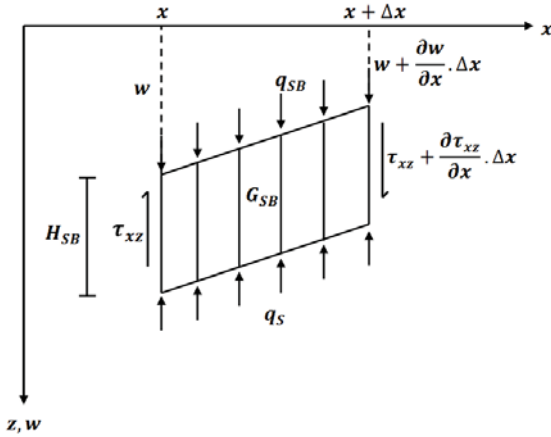


Fig. 6 Free-body diagram of sub-ballast shear layer subjected to stress

The subgrade has been idealised as a burger element which is a combination of Maxwell element and Kelvin-Voigt element applied in series (Selvadurai, 1979). The stress-displacement response of the soft soil subgrade based on the Burger model has been derived as follows,

$$q_s = \frac{w}{A} - T \frac{d^2 w}{dx^2} \quad (18)$$

where,  $T$  is the tensile force per unit length mobilised in the membrane and  $w$  is the deflection of the soil.

The expression for  $A$  is,

$$A = \frac{1}{k_1} + \frac{t}{\eta_1} + \frac{1}{k_2} \left( 1 - \exp\left(-\frac{k_2 t}{\eta_2}\right) \right) \quad (19)$$

where,  $k_1$  is the elastic coefficient of Maxwell model,  $k_2$  is the elastic coefficient of Kelvin-Voigt model,  $\eta_1$  is the viscous coefficient of the Maxwell model,  $\eta_2$  is the viscous coefficient of the Kelvin-Voigt model and  $t$  is the time.

Replacing  $q_s$  in equation 17 with equation 18, the following equation is obtained,

$$q_{SB} = \frac{w}{A} - T \frac{d^2 w}{dx^2} - G_{SB} H_{SB} \frac{\partial^2 w}{\partial x^2} \quad (20)$$

Replacing  $q_{SB}$  in equation 14 with equation 20,

$$q_B = \bar{X}_1 \left( \frac{w}{A} - T \frac{d^2 w}{dx^2} - G_{SB} H_{SB} \frac{\partial^2 w}{\partial x^2} \right) - \bar{X}_2 (T_p + T) \cos \theta \frac{\partial^2 w}{\partial x^2} \quad (21)$$

Combining equations 5 and 21, the final governing equation for the system is obtained as,

$$q = \bar{X}_1 \frac{w}{A} - \left\{ G_B H_B + \bar{X}_2 (T_p + T) \cos \theta + \bar{X}_1 T + \bar{X}_1 G_{SB} H_{SB} \right\} \left( \frac{d^2 w}{dx^2} \right) \quad (22)$$

In order to get the variation of the mobilised tension in the stretched rough membrane, equations 8 and 10 are divided by  $\sin \theta$  and  $\cos \theta$  respectively and added to get the equation given,

$$\frac{\partial T}{\partial x} = -\bar{X}_3 q_B - \bar{X}_4 q_{SB} \quad (23)$$

where,

$$\bar{X}_3 = \mu_R \cos \theta (1 + K \tan^2 \theta) - (1 - K) \sin \theta \quad (24)$$

and

$$\bar{X}_4 = \mu_{SR} \cos \theta (1 + K \tan^2 \theta) + (1 - K) \sin \theta \quad (25)$$

Substituting equations 5 and 20 into equation 23, it turns out that,

$$\frac{\partial T}{\partial x} = -\bar{X}_3 \left( q + G_B H_B \frac{\partial^2 w}{\partial x^2} \right) - \bar{X}_4 \left( \frac{w}{A} - T \frac{d^2 w}{dx^2} - G_{SB} H_{SB} \frac{\partial^2 w}{\partial x^2} \right) \quad (26)$$

## Method of Solution

The response of the proposed foundation model is governed by the equations 22 and 26.

Using non-dimensional parameters,

$$X = \frac{x}{B}, W = \frac{w}{B}, G_B^* = \frac{G_B H_B}{k_S B^2}, G_{SB}^* = \frac{G_{SB} H_{SB}}{k_S B^2}$$

$$q^* = \frac{q}{k_S B}, T_p^* = \frac{T_p}{k_S B^2}, T^* = \frac{T}{k_S B^2}, A^* = k_S A$$

in the equation 22 and 26, and solving subsequently using finite difference formulation can yield settlement response and mobilized tension as

$$q_i^* = \bar{X}_{1i} \frac{W_i}{A^*} - \left\{ G_B^* + \bar{X}_{2i} (T_p^* + T_i^*) \cos \theta_i + \bar{X}_{1i} T_i^* + \bar{X}_{1i} G_{SB}^* \right\} \left( \frac{W_{i-1} - 2W_i + W_{i+1}}{(\Delta X)^2} \right) \quad (27)$$

$$T_i^* = T_{i+1}^* + \left( \frac{\Delta X}{4} \right) \left[ (\bar{X}_{3i} + \bar{X}_{3_{i+1}}) \left\{ (q_i^* + q_{i+1}^*) + G_B^* \left( \left| \frac{\partial^2 W}{\partial X^2} \right|_i + \left| \frac{\partial^2 W}{\partial X^2} \right|_{i+1} \right) \right\} + (\bar{X}_{4i} + \bar{X}_{4_{i+1}}) \left\{ \frac{W_i + W_{i+1}}{A^*} - T_i^* \left( \left| \frac{\partial^2 W}{\partial X^2} \right|_i + \left| \frac{\partial^2 W}{\partial X^2} \right|_{i+1} \right) \right\} - G_{SB}^* \left( \left| \frac{\partial^2 W}{\partial X^2} \right|_i + \left| \frac{\partial^2 W}{\partial X^2} \right|_{i+1} \right) \right] \quad (28)$$



The solution for un-reinforced railway track system was formulated in the similar way and the solution is given in equation 29

$$q_i^* = \frac{W_i}{A^*} - (G_B^* + G_{SB}^*) \left[ \frac{W_{i-1} - 2W_i + W_{i+1}}{(\Delta X)^2} \right] \quad (29)$$

### Boundary and Loading Conditions

Due to symmetry of the system only half portion is taken into consideration. Taking the origin to be at the centre of the loaded region, then, for the edge of the uniformly distributed loading,  $X=1.0$  or  $x=B$ . At the edge of the soil zone, one can see that  $X=L/B$  or  $x=L$ . Due to the symmetry of the problem, the slope of settlement will be zero at  $X=0$ . Also, at  $X=L/B$ , shear stress acting on the shear layer at the edge will be zero due to no confinement. Thus, the boundary conditions can be summarized as follows:

$$\frac{dW}{dX} = 0 \quad \text{at } X = 0 \quad (30)$$

$$\frac{dW}{dX} = 0 \quad \text{at } X = L/B \quad (31)$$

Also, a third boundary condition arises due to very small magnitude of the mobilized tensile force at the edge of the reinforcement.

$$T^* = 0 \quad \text{at } X = L/B \quad (32)$$

The loading condition that are considered are given as:

$$q_i^*(X) = q^* \quad \text{for } |X| \leq 1.0 \quad (33)$$

$$q_i^*(X) = 0 \quad \text{for } |X| > 1.0 \quad (34)$$

## RESULTS AND DISCUSSIONS

A computer program based on the above formulation has been developed using Matlab. Table 1 lists the properties of various components of railway track used in the present study.

Table 1 Properties of Various Components of Railway Track

Parameter	Value
Shear Modulus of Ballast, $G_B$ , MPa	21
Height of Ballast, $H_B$ , m	0.3
Shear Modulus of Sub-Ballast, $G_{SB}$ , MPa	28.75
Height of Ballast, $H_{SB}$ , m	0.15
Coefficient of friction at geosynthetic interface, $\mu_B$	0.6
Coefficient of friction at geosynthetic interface, $\mu_{SB}$	0.6
$k_1$ , MN/m <sup>3</sup>	30
$k_2$ , MN/m <sup>3</sup>	3
$\eta_1$ , N-days/cm <sup>2</sup>	30000
$\eta_2$ , N-days/cm <sup>2</sup>	3000

### Convergence Study

A convergence study was done to obtain optimum number of elements into which the beam shall be divided. The convergence criterion adopted for obtaining the solutions is,

$$\left| \frac{W_i^k - W_i^{k-1}}{W_i^k} \right| \times 100\% < \epsilon_s \quad (35)$$

for all  $i$ , where  $k$  and  $k-1$  denote the present and the previous iterations respectively.  $\epsilon_s$  is the specified tolerance which has taken to be 0.0001 in the present study. Figure 7 shows the convergence study carried out for central deflection.

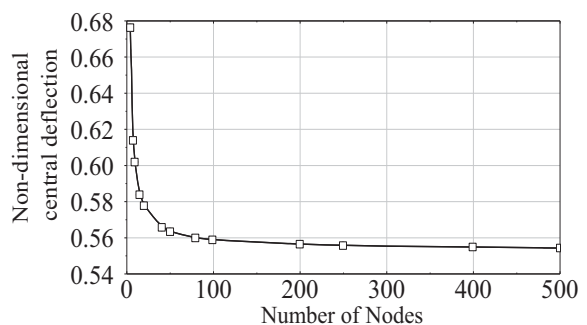


Fig. 7 Central deflection versus number of nodes

### Validation of the Formulation

The formulation made in this study was validated comparing the results with those given by Shukla and Chandra (1994). Shukla and Chandra (1994) developed a formulation in which pre-stressed geosynthetic layer is sandwiched between two Pasternak shear layers, as shown in the Fig. 8. The properties for Burger element were modified considering the properties adopted by Shukla and Chandra (1994).

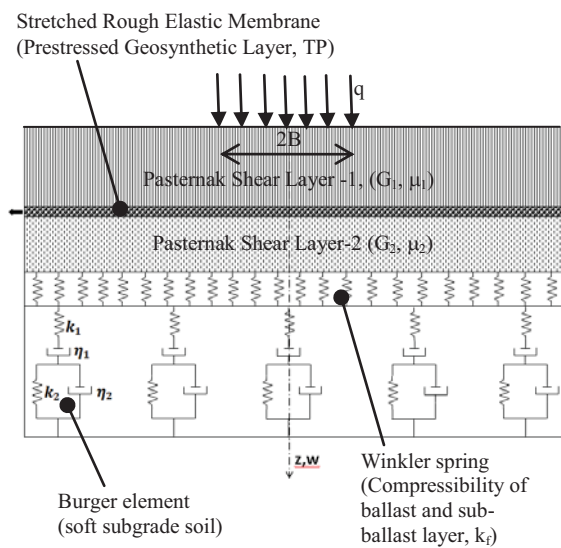


Fig. 8 Schematic diagram of proposed foundation model modified for validation

Figure 9 shows the results of the geosynthetic reinforced system obtained from the present study and Shukla and Chandra (1994). A reasonably good agreement between both the results can be noticed.

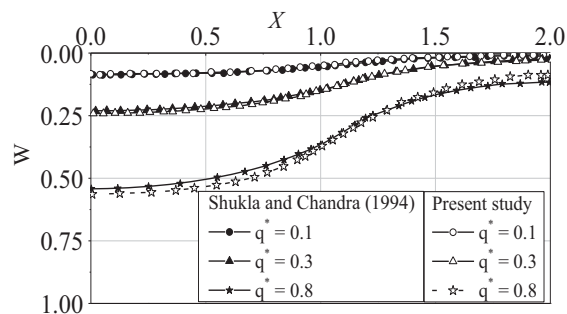


Fig. 9 Validation plot for geosynthetic reinforced foundation system

### Influence of Load on the Settlement Response

The time taken for ultimate consolidation has been determined by calculating settlement profiles at

varying time intervals. For the material properties used in the present study, the variation in the settlement profile was found to be very less when the time period exceeds 15 days, which indirectly suggest that the time taken for ultimate settlement was 15 days. The influence of load on the settlement response was studied by varying the wheel load from 50 tonnes to 250 tonnes at 15 days of consolidation. Typical design loads for passenger trains is around 50 tonnes, however, due to increasing interests in fast moving trains, the design loads are expected to touch around 250-300 tonnes. Figure 10 shows the effect of increasing load on the settlement response of the unreinforced system. It can be noticed that with an increase in the wheel load settlement also increases.

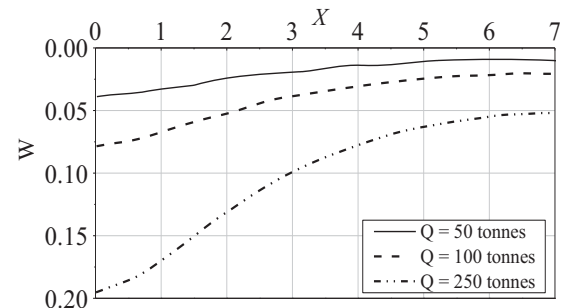


Fig. 10 Variation of settlement along the length of the track under varying loads for unreinforced case

### Influence of Geosynthetic Reinforcement

Figure 11 shows the settlement response of the geosynthetic reinforcement ballasted railway track. With the inclusion of geosynthetic reinforcement between ballast layer and sub-ballast layer, the settlement was found to reduce irrespective of magnitude of the load. The reduction in the settlement is mainly due to the mobilization of the tensile load of the geosynthetic layer.

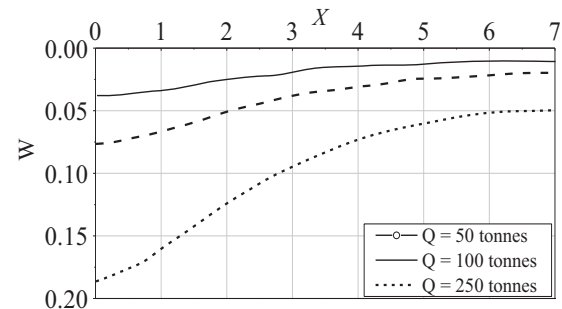


Fig. 11 Variation of settlement along the length of the track under varying loads for reinforced case

Figure 12 shows the variation of the generated mobilized tensile load of geosynthetic layer at various load intensity. As the load intensity were applied only on the sleeper width, uniform mobilization of tensile load can be noticed, however due to the absence of loading in between sleepers, a step-wise mobilization can be noticed.

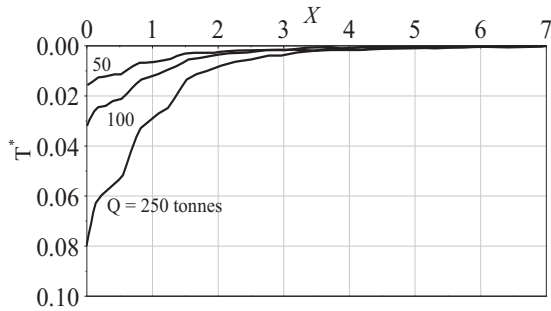


Fig. 12 Effect of varying loads on mobilized tension

## CONCLUSIONS

A foundation model which idealizes a ballasted railway track along with geosynthetic reinforcement considering soft clay as founding soil has been developed in the present study. The developed model has been successfully validated through a literature. The burger model has been used to characterize the soft viscoelastic subgrade.

Numerical solutions have been obtained by adopting the finite difference method combined with non-dimensionalizing the governing equations of the proposed model. It was observed that at a wheel load of 250 tonnes, there is a reduction of 4.9% in the settlement of the reinforced system when compared with the settlement values of the unreinforced system. The reduction in the settlement is due to the mobilized tensile load of geosynthetic provided in between ballast and sub-ballast layers.

## REFERENCES

- Alpan, I. (1967). The empirical evaluation of the coefficient  $K_0$  and  $K_{OR}$ , Soils and Foundations, 7(1): 31-40.
- Beranek, D. (2000). Railway Design and Rehabilitation. US Army Corps of Engineers.
- Selvadurai, A.P.S. (1979). Elastic Analysis of Soil-Foundation Interaction, Elsevier Science Pub. Co., Amsterdam.
- Shukla, S. K. (1995). Foundation Model for Reinforced Granular Fill-Soft Soil System and its Settlement Response. Ph.D. Thesis, Department of Civil Engineering, Indian Institute of Technology, Kanpur, India.
- Shukla, S.K. Chandra, S. (1994). A generalized mechanical model for geosynthetic-reinforced foundation Soil. Geotextiles and Geomembranes, 13(12): 813-825.